

<https://doi.org/10.31891/2307-5732-2026-361-12>

УДК 62-83:681.5.07

БОЛОКАН ОЛЕКСАНДР

Одеський національний технологічний університет

<https://orcid.org/0009-0006-7486-4444>

e-mail: mister.bolokan39@gmail.com

БУКАРОС АНДРІЙ

Одеська військова академія

<https://orcid.org/0000-0002-6306-0874>

e-mail: andrey.bucaros@gmail.com

ПІДВИЩЕННЯ РОБАСТНОСТІ СПОСТЕРІГАЧА СТАНУ ЕЛЕКТРОПРИВОДУ

У статті обґрунтовано доцільність удосконалення адаптивного спостерігача стану електроприводів систем наведення зенітних ракетних комплексів для забезпечення їх ефективного функціонування в режимі перевищення номінальної швидкості обертання виконавчого двигуна, а також для підвищення загальної швидкодії системи наведення. Проаналізовано структуру відомого адаптивного спостерігача стану, реалізованого на основі спостерігачів Люнберґера та застосовуваного в електроприводах бойових машин. Висунуто припущення щодо можливої недостатньої придатності такої структури для роботи електроприводу в зоні підвищених швидкостей. Синтезовано та модернізовано структуру спостерігача стану електроприводу із застосуванням модального методу, з урахуванням нелінійної характеристики намагнічування виконавчого двигуна. Зазначену характеристику попередньо лінеаризовано та подано у вигляді лінійної залежності коефіцієнта ЕРС та моменту від струму збудження. У середовищі Matlab/Simulink досліджено вплив параметричної невизначеності двигуна постійного струму типу Д-135 на роботу базової структури спостерігача у складі системи наведення зенітного ракетного комплексу 9К35. Результати показали, що така структура демонструє високу стійкість до параметричних відхилень, зокрема зміни активного опору обмотки якоря та моменту інерції, при цьому похибка оцінювання кутової швидкості не перевищує 4%. Водночас встановлено, що зі зменшенням магнітного потоку, характерного для роботи електроприводу в діапазоні швидкостей, які перевищують номінальні, базова структура спостерігача повністю втрачає працездатність. Проведено чисельне моделювання роботи вдосконаленого спостерігача стану у складі системи наведення зенітного ракетного комплексу 9К35. Результати моделювання підтвердили його ефективність і забезпечення стабільного функціонування електроприводу в обох зонах швидкості.

Ключові слова: спостерігач Люнберґера, двигун постійного струму, електропривод наведення, зенітний ракетний комплекс.

BOLOKAN OLEKSANDR

Odesa National University of Technology

BUKAROS ANDRII

Odesa Military Academy

IMPROVING THE ROBUSTNESS OF THE ELECTRIC DRIVE STATE OBSERVER

The paper substantiates the feasibility of improving the adaptive state observer of surface-to-air missile systems guidance electric drives in order to ensure their effective operation in mode of exceeding the executive motor nominal rotation speed, as well as to increase the overall speed of the guidance system. The structure of the well-known adaptive state observer, implemented on the basis of Luenberger observers, which is used in electric drives of combat vehicles, is analyzed. A hypothesis is put forward regarding its potential unsuitability when the electric drive operates in the zone of increased speeds. The structure of the electric drive state observer is synthesized and modernized using the modal method, taking into account the nonlinear characteristic of the executive motor magnetization. This characteristic was previously linearized and presented in the form of a linear dependence of the EMF coefficient and torque on the excitation current. The influence of the parametric uncertainty of the direct current motor type D-135 on the operation of the basic observer structure as a part of the 9K35 surface-to-air missile guidance system was studied by simulation in the Matlab/Simulink environment. The results showed that such a structure demonstrates high robustness to deviations in the active resistance of the armature winding and the moment of inertia, while the error in estimating the rotational speed does not exceed 4%. At the same time, when the magnetic flux corresponding to the operation of the electric drive in the speed range higher than the nominal one decreases, a complete loss of the basic observer structure operability was detected. Numerical simulation of the operation of the improved state observer as part of the 9K35 surface-to-air missile guidance system was carried out. The simulation results confirmed its effectiveness and stable operation of the electric drive in both speed modes.

Keywords: Luenberger observer, DC motor, guidance electric drive, surface-to-air missile system.

Стаття надійшла до редакції / Received 13.12.2025

Прийнята до друку / Accepted 11.01.2026

Опубліковано / Published 29.01.2026



This is an Open Access article distributed under the terms of the [Creative Commons CC-BY 4.0](https://creativecommons.org/licenses/by/4.0/)

© Болокан Олександр, Букарос Андрій

Problem statement

Direct current (DC) motors are widely used in electric drives of both modern military equipment and existing weapons of the last century: self-propelled guns and navigation systems (Wylie, 2025), multiple launch missile systems (Paranchuk et al., 2018), surface-to-air missile systems (Saputra et al., 2015; Tata Advanced Systems, n.d.), missile fin actuation systems (Ghadi, 2022), automotive and engineering equipment (Reimers, 1973). Guidance electric drives of surface-to-air missile systems (SAMS) are usually equipped with closed-loop speed control systems of executive electric motors (Somefun et al., 2020), which provides automated guidance to an air target. In such systems, speed sensors are widely used, among which the most common are DC tachogenerators. However, the use of these sensors significantly affects the dynamic characteristics of closed-loop control systems, in particular, the speed of the guidance process. The latter parameter is critically important given the tactical and technical requirements for SAMS in combat conditions, where the speed of response to a threat is of crucial importance.

Literature overview

To solve this problem, it is advisable to use methods for sensorless estimation of the guidance system actuator motor rotational speed. Among such approaches, Kalman filters (Rigatos & Siano, 2011) and adaptive state observers (Abut, 2018) are distinguished. In (Bukaros et al., 2022), a comparative analysis of the above methods was carried out, on the basis of which the advantages of using Luenberger observers (LO) in DC electric drives were substantiated. Similar results (Sadhu & Ghoshal, 2011) are given in the study, which demonstrated the effectiveness of using LO in homing systems of guided missiles. Therefore, it is advisable to use LO to implement control systems for SAMS guidance electric drives.

The theoretical foundations of Luenberger observers (LO) were thoroughly developed back in the 20th century, and their practical application, in particular in DC electric drive systems, has been confirmed by a number of research works considered earlier. These developments are based on the assumption of constancy of the actuator motor parameters during its operation. At the same time, the relevance of increasing the speed of the guidance process determines the need to find more effective methods of controlling the motor speed. One of the promising directions is the use of two-zone control systems (Fitzgerald et al., 2002), which allow increasing the motor speed by weakening the magnetic flux. On this basis, a scientific hypothesis can be formulated: with significant changes in the magnetic flux in a DC motor, traditional SO structures may lose their performance and require appropriate modernization.

Purpose of the article

The aim of the research is to create an adaptive state observer for guidance electric drives of SAMS with robustness properties to changes in the magnetic flux of the executive motor. The introduction of such an observer opens up the possibility of implementing two-zone control of the engine speed, which will contribute to improving the dynamic characteristics of the guidance system.

Materials and methods

The analysis of the LO with the known structure will be carried out using the example of the horizontal guidance electric drive of the SAMS 9K35 (Fig. 1).

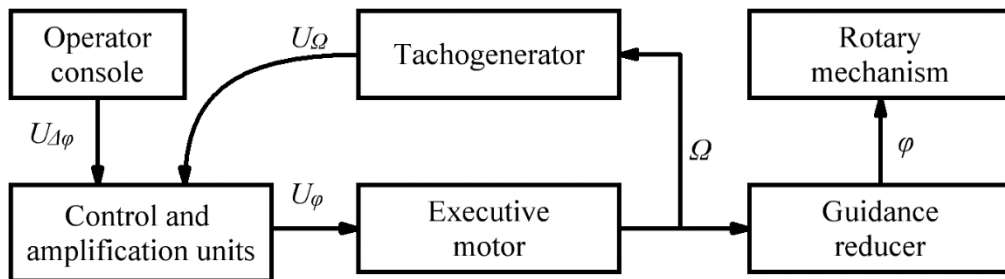


Fig. 1. Horizontal guidance system of the SAMS 9K35

Fig. 1 shows: φ is the horizontal guidance angle; Ω is the rotational speed of the motor; U_{φ} is the control voltage; $U_{\Delta\varphi}$ is the target azimuth signal; U_{Ω} – feedback signal based on the rotational speed of the motor. As can be seen from Fig. 1, in the specified electric drive, feedback on the rotational speed of the executive DC motor with independent excitation of the D-135 type is implemented, which is carried out using a tachogenerator.

In (Bukaros et al. 2022), the synthesis of the LO with the distribution of the characteristic polynomial roots according to the linear Chebyshev form was performed. The diagram of the synthesized system, presented in Fig. 2, provides the ability to estimate both the rotational speed and the resistance moment on the shaft of the executive DC motor D-135 in real time.

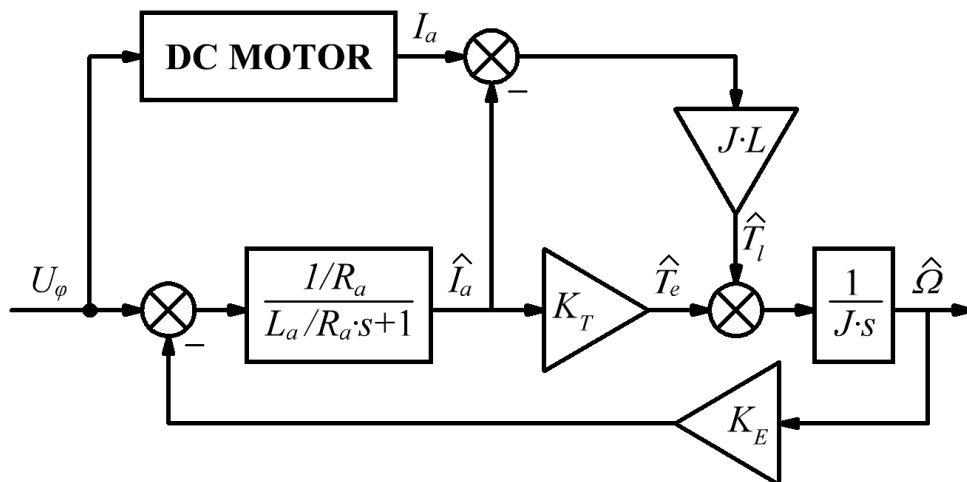


Fig. 2. Block diagram of a known LO

Fig. 2 shows: I_a, \hat{I}_a are respectively measured and estimated value of the armature current; $\hat{\Omega}$ is the estimated value of the motor rotation speed; R_a, L_a are respectively the active resistance and inductance of the armature winding; \hat{T}_e, \hat{T}_l are respectively estimated values of the electromagnetic and load torque; J – moment of the armature inertia; K_T, K_E – respectively the torque and voltage constants; s – Laplace variable; L – coefficient of the Luenberger matrix.

It is known that when the DC motor operates in the speed range below the nominal (single-zone control mode), the armature resistance R_a changes by several percent due to Joule heat generation (Furuta et al., 2024). In the case of using the DC motor as part of an electric drive with a displacement or rotation mechanism, the total moment of inertia J , reduced to the electric drive shaft, can change significantly. To transition the motor to the operating mode at a speed exceeding the nominal (two-zone control), it is necessary to reduce the magnetic flux Φ . Thus, when analyzing the robustness properties of the LO, we will consider as variable parameters of the DC motor: the armature winding resistance (with a deviation of up to 10%), the moment of inertia reduced to the motor shaft (with a deviation of up to 100%), and the motor magnetic flux (with a deviation of up to 50%).

According to the scientific hypothesis put forward in the introduction, the LO with a known structure (Fig. 2), having robustness properties with respect to the parameters of the DC motor, will lose its operability with significant changes in the motor magnetic flux. To eliminate this drawback, it is proposed to improve the known LO by structural changes.

The system of equations describing the mathematical model of the known LO can be written as follows:

$$\begin{cases} \frac{d}{dt} \widehat{M}_e = -\frac{R_a}{L_a} \widehat{M}_e - \frac{K^2}{L_a} \widehat{\Omega} + \frac{K}{L_a} U_\varphi \\ \frac{d}{dt} \widehat{\Omega} = \frac{1}{J} \widehat{M}_e + L(I_a - \hat{I}_a) \end{cases} \quad (1)$$

where $K = K_T = K_E$ is the DC motor constant.

Equations (1) are built on the assumption of the DC motor magnetic flux Φ constancy, and accordingly, the coefficient K . In the case of the DC motor operation in the second speed zone, where the magnetic flux is weakened, it is necessary to introduce the dependence $K=f(\Phi)$ into equations (1). At the same time, it should be taken into account that to determine the value of Φ in real time, it is necessary to integrate Hall sensors into the design of the executive motor, which significantly complicates the electric drive and contradicts the aim of the study. As an alternative solution, it is proposed to measure the field current I_f using a simple sensor, and include the dependence $K=f(I_f)$ in equations (1). This dependence is generally nonlinear and is determined by the magnetization curve of the DC motor (Fitzgerald et al., 2002). Since the LO is robust to minor changes in the parameters of the observed object (Abut 2018, 70), it is permissible to linearize this dependence and present it in the form $K = L_{af} \cdot I_f$, where L_{af} is the field-armature mutual inductance.

Thus, equation (1) can be rewritten as

$$\begin{cases} \frac{d}{dt} \widehat{M}_e = -\frac{R_a}{L_a} \widehat{M}_e - \frac{L_{af}^2}{L_a} I_f^2 \cdot \widehat{\Omega} + \frac{L_{af}}{L_a} I_f \cdot U_\varphi \\ \frac{d}{dt} \widehat{\Omega} = \frac{1}{J} \widehat{M}_e + L(I_f) \cdot (I_a - \hat{I}_a) \end{cases} \quad (2)$$

Equation (2) corresponds to the structural diagram of the LO, which is shown in Fig. 4.

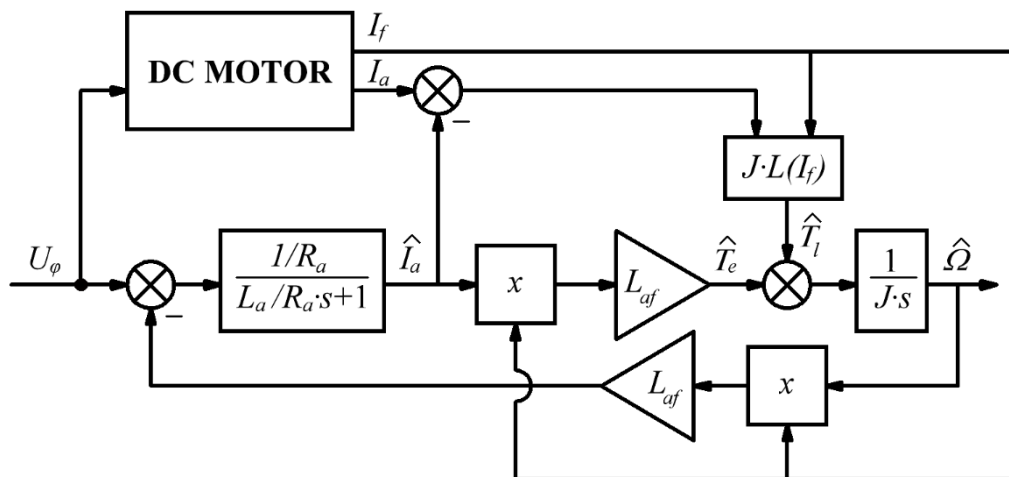


Fig. 3. Block diagram of a modernized LO

As shown in Fig. 3, the modernized observer is implemented using only two current sensors - the armature I_a and the field I_f of the DC motor. This design provides the possibility of real-time estimation of the motor torque T_e , the shaft load moment T_l and the angular velocity Ω . The corresponding expression for the coefficient of the Luenberger matrix has the following form:

$$L(I_f) = \frac{1}{J} - \frac{R_a^2}{L_a \cdot (A_1 \cdot L_{af} \cdot I_f)^2} \quad (3)$$

where A_1 is the form factor (Bukaros et al., 2022).

Based on the structural diagram in Fig. 3, a simulation model was created in the Matlab/Simulink environment, which is shown in Fig. 4.

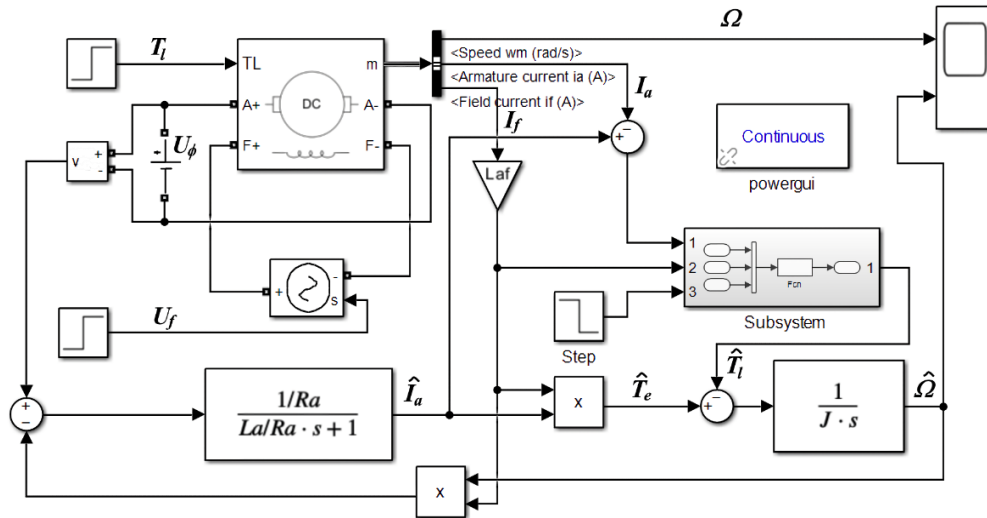


Fig. 4. Simulation model of a modernized LO

In the model presented in Fig. 4, the mechanism for weakening the magnetic flux of the D-135 motor is implemented using the U_f signal, which simulates the field voltage. The T_l signal reproduces the pulse load on the motor shaft, which is typical for real electromechanical systems due to the presence of backlash. The \hat{T}_l signal is used to simulate the estimated load moment on the motor shaft. The Ω signal reflects the current angular velocity of rotation of the motor. The powergui block is responsible for setting the initial conditions for the simulation. The calculation of the Luenberger matrix coefficient according to formula (3) is performed in the Subsystem block, while the Step block prevents the occurrence of division by $I_f = 0$, which can occur at the beginning of the simulation with zero initial conditions. All other signals and blocks of the model correspond to the structural diagram shown in Fig. 3.

Before the start of experimental studies, the model presented in Fig. 4 was initialized according to the passport characteristics of the D-135 type DC motor. To ensure maximum system performance, the A_1 form factor was set at 1.38.

The numerical experiment was carried out in 3 stages. At the first stage, the U_f signal was set to the nominal value, which corresponds to the operation of the electric drive in the first speed zone. During the simulation, the motor parameters were changed, such as the active resistance of the armature winding with an increase of 10%, the moment of inertia, brought to the motor shaft with a decrease of 100%.

In the second stage of the experiment, at 5 seconds, the U_f signal was abruptly reduced by 2 times to simulate the weakening of the motor magnetic flux which corresponds to the operation of the electric drive in the second speed zone. At the same time, the value of the field current signal I_f supplied to the LO blocks remained unchanged and equal to the nominal value.

In the third stage of the experiment, the change in the I_f signal was taken into account.

Results and discussion

The results of the first stage of the experiment are shown in Fig. 5a and 5b. The results of the second and third stages of the experiment are shown in Fig. 5c and 5d, respectively.

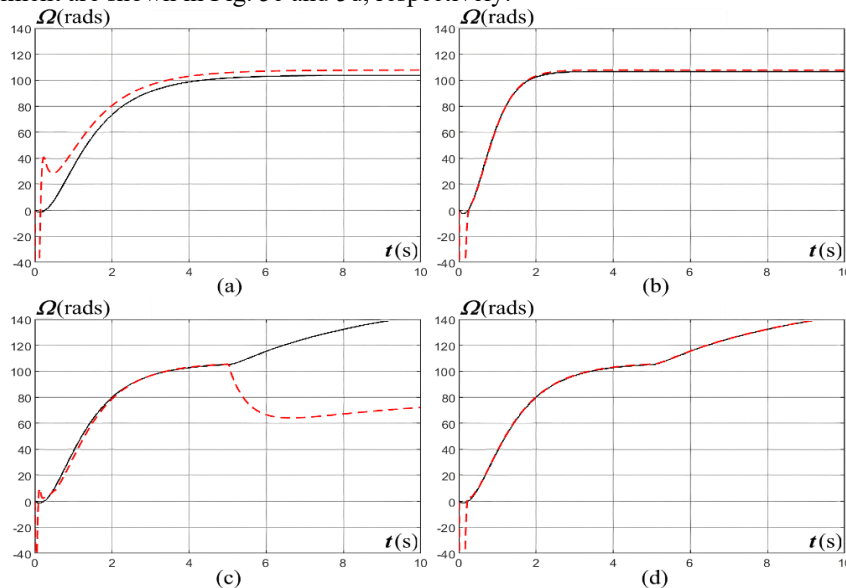


Fig. 5. Simulation results

In Fig. 5, solid lines show the angular velocity curves of the studied motor, which are obtained from the MATLAB model of the DC motor. Dashed lines indicate the angular velocity estimation curves obtained from the LO model.

Analysis of the graphs presented in Fig. 5a and 5b indicates the high robustness of the known LO with respect to changes in the active resistance of the armature winding and the moment of inertia of the electric drive. In particular, after the observer adaptation process is completed at 0.8 seconds, the error in estimating the angular velocity does not exceed 4% when the armature winding resistance is increased by 10%, and 1% when the moment of inertia is reduced by 2 times, which confirms the effectiveness of the algorithm in conditions of parametric changes in the system and does not require its improvement.

If the magnetic flux of the motor is reduced by 50% and the electric drive moves to the second speed control zone (Fig. 5c), the efficiency of the known LO is significantly reduced, which actually indicates its inability to provide a correct estimate of the rotation speed. The results obtained confirm the previously formulated scientific hypothesis regarding the limitations of the use of the known LO in the specified mode of the electric drive operation.

Fig. 5d presents the results of numerical simulations, which demonstrate the full functional suitability of the improved LO in both speed control zones of the electric drive. After a short adaptation interval of 0.3 s, the estimate of the motor angular velocity follows the real value quite accurately, with an error not exceeding 1%.

Conclusions

Based on the research conducted, the following conclusions can be formulated.

The results of the experiment confirmed the effectiveness of the proposed structure of the improved LO. The developed LO provides sensorless estimation of the DC motor angular velocity in conditions of two-zone speed regulation, while the error does not exceed 1%. Such accuracy allows integrating this observer into the guidance electric drives of surface-to-air missile systems, contributing to the improvement of the dynamic characteristics of the guidance process.

The simulation model of the improved LO also provides the ability to estimate the load torque on the motor shaft. This, in turn, creates the prerequisites for the development of robust control systems that are resistant to the effects of backlash and elastic couplings typical of electromechanical systems.

The proposed model requires further improvement and research, since its structure includes signal multiplication blocks, which, if there is a measurement error in at least one of the arguments, can cause a multiplicative error in the process of estimating the parameters of the motor. Such an effect can negatively affect the accuracy and stability of the system in real operating conditions.

References

1. Abut, T. (2018). Control of a DC motor using sensorless observer based sliding mode control method. *International Journal of Engineering Trends and Technology*, 66(2), 67–72. <https://doi.org/10.14445/22315381/ijett-v66p212>
2. Bukaros, A., Herega, A., Sergeiev, V., Obnyavko, T., & Konkov, K. (2022). State observer of the combat vehicle electric drives. *Collection of Scientific Works of Odesa Military Academy*, 1(17), 116–124. <https://doi.org/10.37129/2313-7509.2022.17.116-124>
3. Fitzgerald, A. E., Kingsley, C., Jr., & Umans, S. D. (2002). *Electric machinery* (6th ed.). McGraw-Hill Science/Engineering/Math.
4. Furuta, S., Koshibae, W., Matsuura, K., et al. (2024). Reconsidering nonlinear emergent inductance: Time-varying Joule heating and its impact on AC electrical response. *Physical Review B*, 110(17), 174402. <https://doi.org/10.1103/physrevb.110.174402>
5. Ghadi, P. (2022, April 28). DC motors for missile fin actuation systems. *Portescap*. <https://www.portescap.com/en/newsroom/blog/2022/04/dc-motors-for-missile-fin-actuation-systems>
6. Paranchuk, Y., Evdokimov, P., Koziy, V., & Tsjapa, V. (2018). Mathematical modelling and experimental determination of parameters of the guidance system of weaponry complex. *Computational Problems of Electrical Engineering*, 8(2), 73–78. <https://doi.org/10.23939/jcpee2018.02.073>
7. Reimers, E. (1973). An application of two-phase DC chopper motor drive. *IEEE Transactions on Industry Applications*, IA-9(3), 285–293. <https://doi.org/10.1109/tia.1973.349905>
8. Rigatos, G. G., & Siano, P. (2011). Sensorless control of electric motors with Kalman filters: Applications to robotic and industrial systems. *International Journal of Advanced Robotic Systems*, 8(6), 71. <https://doi.org/10.5772/10680>
9. Sadhu, S., & Ghoshal, T. K. (2011). Sight line rate estimation in missile seeker using disturbance observer-based technique. *IEEE Transactions on Control Systems Technology*, 19(2), 449–454. <https://doi.org/10.1109/tcst.2010.2046662>
10. Saputra, J., Hasanah, R. N., & Muslim, M. A. (2015). Target tracking of the S-60 single-barrel 57mm anti-aircraft gun system using hybrid control method. *Journal of Engineering and Applied Sciences*, 10(19), 9071–9077. https://www.arpnjournals.org/jeas/research_papers/rp_2015/jeas_1015_2839.pdf
11. Somefun, O., Akingbade, K., & Dahunsi, F. (2020). Speed control of DC motors: Optimal closed PID-loop model predictive control. *Universal Journal of Control and Automation*, 8(1), 9–21. <https://doi.org/10.13189/ujca.2020.080102>
12. Tata Advanced Systems. (n.d.). Upgradation of 40mm L70 air defence gun. *Tata Advanced Systems*. Retrieved October 26, 2025, from <https://www.tataadvancedsystems.com/air-defence-gun40mm>
13. Wylie, A. (2025, October 3). Servo motors for military and defense applications. *Defense Advancement*. <https://www.defenseadvancement.com/suppliers/servo-motors-military/>